ReactorSTM : imaging catalysts under realistic conditions

Herbschleb, C.T.

Chapter 4

High-resolution STM imaging: CO oxidation on Pt(110)

4.1 The reaction system: Expectation

The oxidation of CO on transition metal based catalysts has instigated extensive studies [76–82, 124, 125]. These include high-pressure STM studies [124] and high-pressure SXRD studies [125], on several surface orientations of palladium and platinum, one of which is Pt(110). As argued in chapter 2, CO oxidation on Pt(110) has been used primarily as a test reaction for the ReactorSTM Mark II, to determine its performance, with respect to the ReactorSTM Mark I. In addition, this experiment has yielded a few results, unveiling more of the strengths of the ReactorSTM Mark II, in addition to "just" atomic row resolution STM images, in the (1x2) missing-row reconstruction on Pt(110), at room temperature and low vacuum conditions, and atomic row resolution on Pt(110) under a flow of 1 bar of CO at 160℃.

In the aforementioned studies, the reaction system, as modelled in figure 4.1, is proposed to hold for CO oxidation on Pt(110). Figure 4.1 is divided into four phases, which are distinguished by the ratios between the partial pressures of CO and O_2. We start from a clean Pt(110) surface, exhibiting its (1x2) missing-row reconstruction (fig. 4.1 A), as has been observed in STM imaging [128]. After exposure to CO, following arrow 1 in figure 4.1, the reconstruction is lifted, and the surface restructures into its (1x1) phase. Due to the half-occupation of the outermost layer, resulting from the 1x2 to 1x1 transition, initially a pattern of (1x1) patches, which have the Pt(110) monatomic step height of 1.4 Å, with respect to the layer below, is formed on the surface. This resembles the pattern of the skin of a tiger, hence the

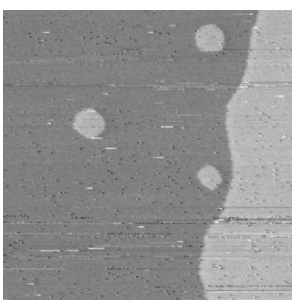

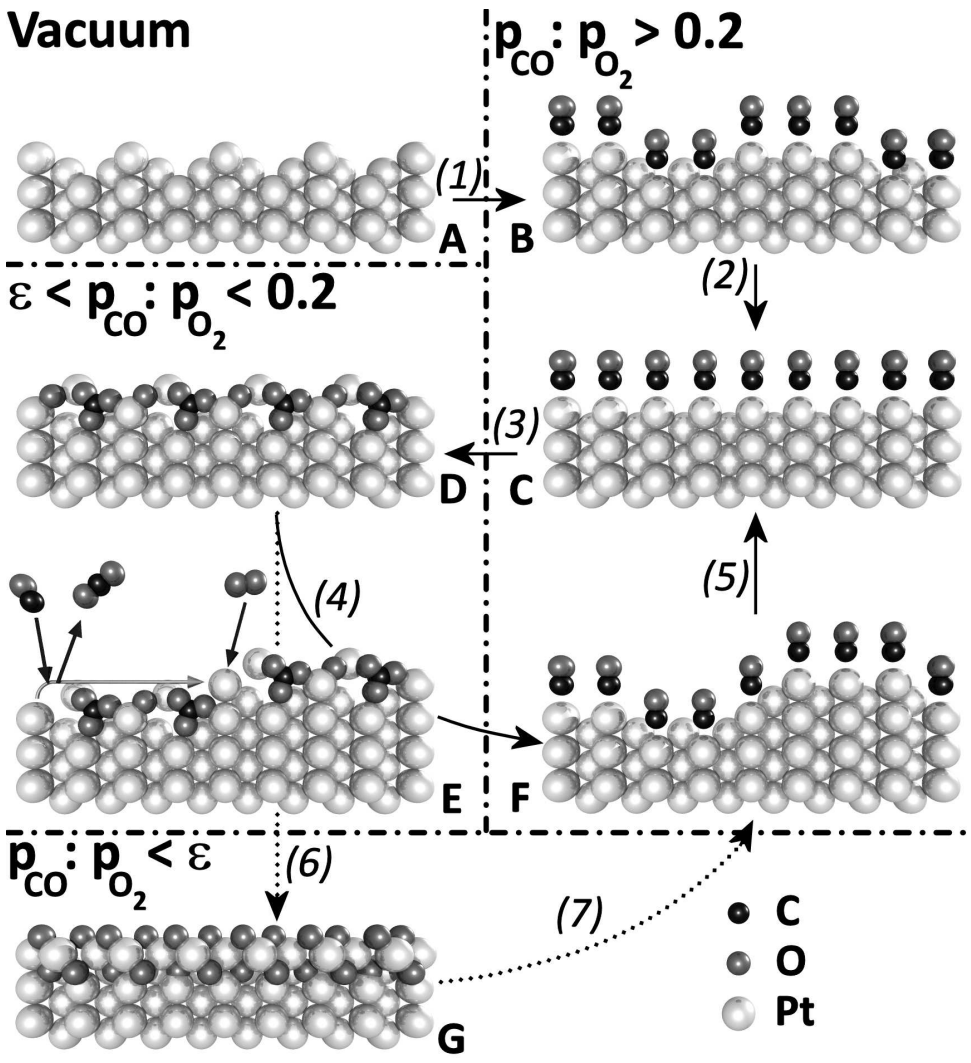

Figure 4.1: A model for the CO-oxidation reaction system on Pt(110). There are four phases distinguished by certain $p_{CO} : p_{O_2}$ values. (A) (1x2) missing-row reconstruction under vacuum. (B) The tiger skin pattern after CO-exposure of (A). (C) The flat, CO-covered metallic surface. (D) (1x2) commensurate oxide structure, including carbonate ions. (E) The Mars-Van Krevelen mechanism in action. (F) The rough CO-covered metallic surface. (G) α-PtO_2.

"tiger skin" pattern, which is observed in STM images [124, 127] (4.1 B). In time (arrow 2), surface diffusion leads to a flat, CO-covered metallic surface (4.1 C), which is the equilibrium situation in a CO-rich phase. This results in STM images showing large terraces, which have the Pt(110) monatomic step

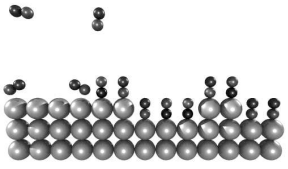

height. When $p_{CO} : p_{O_2}$ is changed to roughly < 0.2 (arrow 3), the surface undergoes a phase transition into a (1x2) commensurate oxide structure (4.1 D). Although this structure has never been atomically resolved in real space, the (1x2) period has been observed in reciprocal space by SXRD [125]. Since no known platinum oxide terminates in this (1x2) commensurate shape on the surface, and the (1x2) missing-row reconstruction is excluded by the fact that the rows of the new structure are shifted in the (001) direction, it has been suggested by DFT calculations that carbonate ions are involved in this structure. This, in turn, explains why this structure *only* occurs when there are significant traces of CO present in the gas atmosphere. The carbonate ions might act as an intermediate in the CO_2 formation. Large scale STM images have indicated that the surface, in this case, becomes progressively rougher with respect to the metallic phase; patches, with a height of 2 to 4 Å and a width of 4 to 7 nm, cover the surface [124]. Since the height of these patches did not correspond with (an integer of) the monatomic step height on Pt(110), they were ascribed to an oxide. The roughening of the surface is ascribed to the active reaction mechanism in this phase, the Mars-Van Krevelen mechanism, which is shown in 4.1 E. A CO molecule reacts with an oxygen atom on the oxide surface to form CO_2, which desorbs, creating an under-coordinated platinum atom on the surface. A certain fraction of these under-coordinated platinum atoms becomes highly mobile, diffusing on the oxide surface, until they get oxidized, and immobilized in the oxygen-rich gas atmosphere. The (1x2) structure, however, was not observed in the earlier mentioned STM images. On the one hand, from the situation in 4.1 D, the CO pressure can be increased again (arrow 4), switching the surface back to the CO-covered metallic state, which initially will be a rough metallic surface (4.1 F). The roughness, induced by the formation of the oxide layer, will anneal out by diffusion (arrow 5), returning the surface to its equilibrium situation, the flat, metallic surface, as in 4.1 C; this process has been observed by STM [124]. On the other hand, when the pressure ratio $CO:O_2$ drops below ϵ (arrow 6), the (1x2) commensurate oxide is replaced by the incommensurate hexagonal α-PtO_2 oxide (4.1 G), which has been observed in SXRD [125]. Also, due to the Mars-Van Krevelen reaction mechanism, this oxide will slowly roughen. When this (roughened) oxide is again exposed to CO (arrow 7), the surface switches back to the rough CO-covered metallic state (4.1 F), following the same steps as described above.

If there is a clear energy difference between the adsorption of CO onto steps with respect to the terraces, the surface can spontaneously switch from an oxide to a metal at a particular $CO:O_2$ ratio. At the same $CO:O_2$ ratio, a flat metallic surface will oxidize. In the model described in figure 4.1,

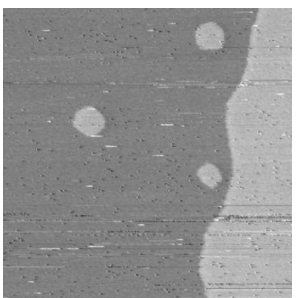

we have shown that the surface roughens in the oxidic state, by the Mars-Van Krevelen reaction mechanism, and smoothes by diffusion in the metallic state. All these ingredients can lead to spontaneous reaction oscillation at the mentioned $CO:O_2$ ratio, which is the case for many of the surface orientations of palladium and platinum. A model for this type of reaction oscillation, linking the evolution of roughness in the oxidic and metallic states, and the affinity of CO binding at steps, is discussed in depth in [28]. In the case of Pt(110), however, reaction oscillation has never been observed. A reason for this might be the existence of the intermediate (1x2) commensurate oxide structure (4.1 D), which does not exist for the other surfaces, destroying the regime in which spontaneous reaction oscillations for the other surface orientations exists.

4.2 The reaction system: Mark II experiments

4.2.1 STM images and reaction kinetics

The results obtained with the ReactorSTM Mark II are summarized in figures 4.2, 4.3, and 4.4. Figure 4.2 shows a series of STM images, with different length scales in various gas compositions, whereas figure 4.3 shows the same phase diagram as figure 4.1, in which the ball models have been replaced by STM images at a fixed length scale of 4.5 nm^2. This way of presenting the STM images has been chosen deliberately. In figure 4.2, the large scale images, representing the various reactor conditions, show important surface properties, such as atomic density and mobility. In addition, the high quality of the z-scale in these particular images allows us to determine the atom-row distance quantitatively, by the use of height profiles, which are also shown in figure 4.2. In the phase diagram, figure 4.3, the length scale of the STM images has been kept constant, which in some of the phases leads to lower quality STM images, with respect to their analogous images shown in figure 4.2. Keeping the length scale constant, however, provides a very clear picture of the atomic level changes which occur when switching from one phase to another. Figure 4.4 shows the reaction kinetics, as measured by the quadrupole mass spectrometer during this experiment.

Figure 4.2 A shows an STM image of the Pt(110) surface, at room temperature in an ill defined vacuum[1]. This image resolves the (1x2) missing-row

[1] As I explained in chapter 2, the reactor volume is separated from the ultrahigh vacuum environment during STM operation, implying that the pressure will slowly increase after the reactor is closed. This means that, prior to exposing the sample to high gas pressures,

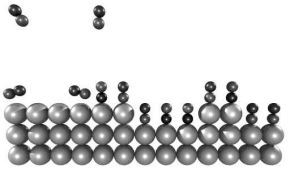

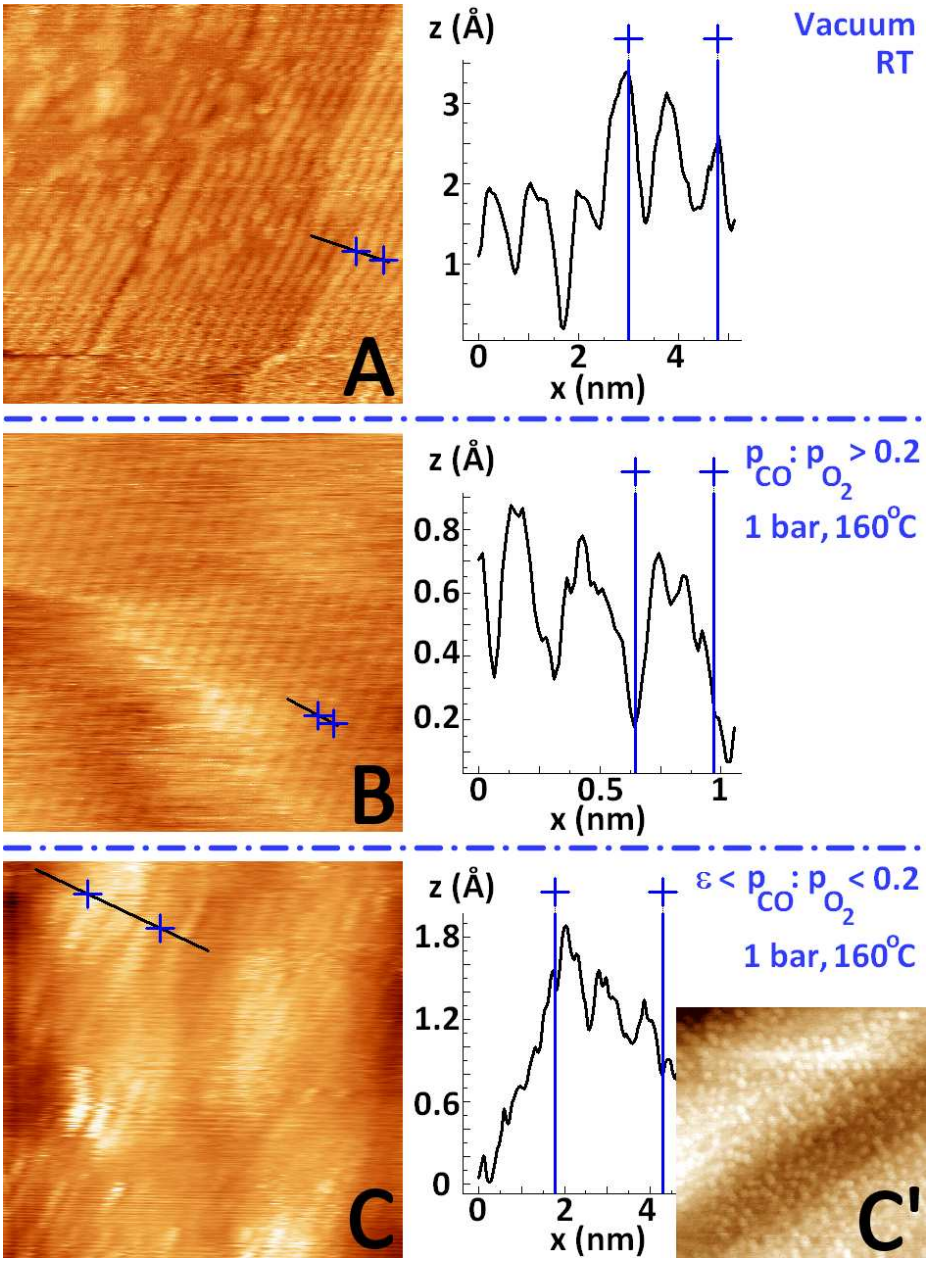

Figure 4.2: STM images and corresponding height profiles in three different phases. (A) A 25 nm x 25 nm STM image of the missing-row reconstruction, at room temperature under vacuum. (B) A 7.5 nm x 7.5 nm STM image of Pt(110), at 160℃ and 1 bar of CO. (C) A 12.5 nm x 12.5 nm STM image of Pt(110), at 160℃ and 1 bar of O_2/CO. (C') A 210 nm x 210 nm STM image of Hendriksen et al. [27], under the same conditions.

the freshly prepared sample will be exposed to the reactor's "bad breath", which will always contain remnants of the gases used in the last experiment, typically influencing the surface structure.

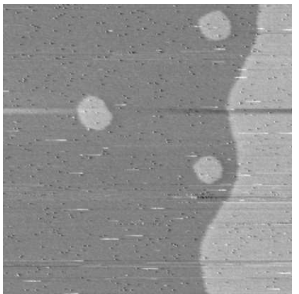

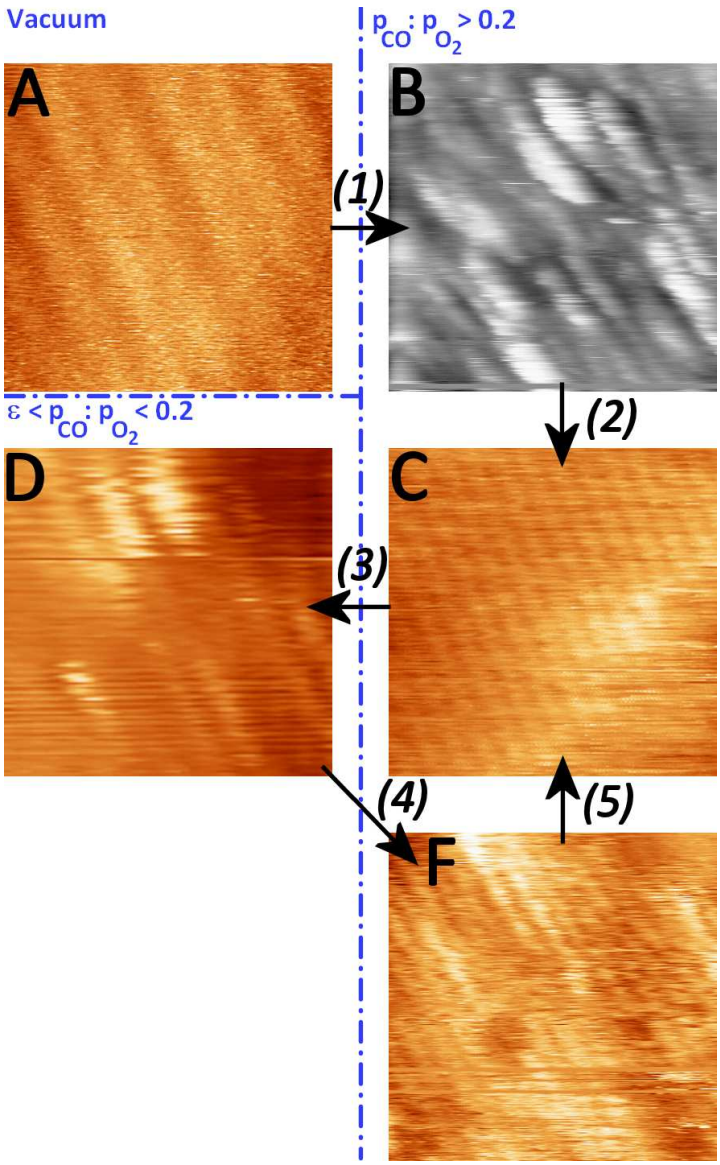

Figure 4.3: A phase diagram, as in figure 4.1, with STM images as obtained with the ReactorSTM Mark II. Unless otherwise stated, $T = 160℃$. All images are 4.5 nm x 4.5 nm, except for the grey scale image (15 nm x 15 nm). (A) The missing-row reconstruction, under vacuum at room temperature. (B) The tiger skin pattern, after exposure of (A) to 1 bar CO. (C) Flat, metallic Pt(110), in a CO-rich flow. (D) Roughened Pt(110), exhibiting the (1x2) commensurate surface oxide, at a high O_2/CO ratio. (F) Rough, metallic Pt(110) in CO-rich flow.

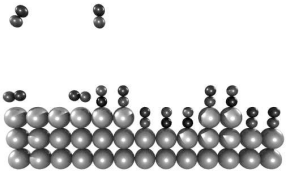

reconstruction, which Pt(110) exhibits in vacuum, after applying standard sample preparation techniques (1 keV Ar^+ ion bombardment, followed by annealing at ∼1000 K). By using height profiles, such as the one corresponding to image A, the average inter-row distance has been measured to be 0.75 ± 0.03 nm. This is consistent with the theoretical value of 0.78 nm [89]. In the upper left hand corner of image A, however, the periodicity conforming with the surface reconstruction is broken: larger clumps of material have accumulated in adatom islands. A reason for this restructuring process is the fact that the ill defined vacuum, to which the sample is exposed in this stage, contains gases, which induce lifting of the reconstruction (see footnote). Finally, from the top right hand to one-third left of the bottom right hand, runs a step with a height of 1.5 Å, corresponding to the monatomic step height on Pt(110) of 1.4 Å [129]. Image B, in figure 4.2, shows an atomic-row resolved STM image of Pt(110), exposed to 1 bar of CO at a temperature of 160℃. In this case, the average row distance is 0.37 ± 0.02 nm, corresponding to the theoretical distance between the rows of the normal (110) surface termination of metallic platinum [90]. This surface is not rigid: in the bottom half of the image, a number of horizontal stripes occur coinciding with the scan direction of the STM. These stripes are not caused by noise or tip effects, but by step dynamics – they cover a step on the surface. The mobility of single atoms at a step, namely, is much higher than the line scan speed of the STM, meaning that every time the STM tip scans over the edge of the step, a different number of atoms will be present at that step, at that particular moment. This will lead to a stripy step, which is what we observe[2]. Finally, image 4.2 C shows an STM image of Pt(110), exposed to 1 bar of a CO/O_2 mixture, with a ratio $\epsilon < p_{CO} : p_{O_2} < 0.2$ at 160 ℃. It can immediately be seen that the roughness on the surface has increased, in the form of the formation of protrusions. Hendriksen et al. [27] have already shown this structural change on the surface by high-pressure STM (image C'), but they could not resolve the atomic details of this structure. By the use of spectroscopic techniques, however, they could determine that the structure on the protrusions was the same as the structure in between the protrusions. Moreover, they ascertained that this structure is not consistent with a metallic state of platinum. As they found, the height of these protrusions, ∼0.2 nm, was not in agreement with the monatomic step height on Pt(110). They also determined the sizes of the protrusions to be between 6 and 8 nm. As I mentioned in the former section, Ackermann et al. [36] have studied this system by high-pressure SXRD, also observing this structure in reciprocal space. Their observation revealed a commensurate structure with a (1x2) period, which they, in combination

[2]Similar work has been done on Au(111) [130, 131]

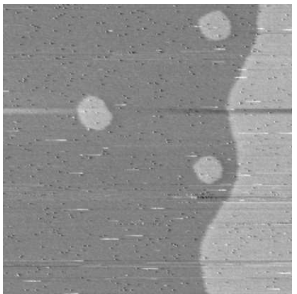

with density functional theory calculations, determined to be a surface oxide, incorporating carbonate ions. Physical proof for these indirect observations, using the ReactorSTM Mark II, has been provided. A commensurate super structure, with an average periodicity of 0.72 ± 0.06 nm has been observed, which indeed agrees with a (1x2) period. Furthermore, this period has been observed both on the protrusions (of which four are visible in image C), and in between the protrusions, supporting both Hendriksen's and Ackermann's results.

The phase diagram, shown in figure 4.3, shows the full cycle of the Pt(110) surface during an experiment. It has been built up in the same way as figure 4.1, labelling the STM images and arrows between the phases, in figure 4.3, with the same letters and numbers as the ball models and arrows in figure 4.1. The length scales of the STM images are now all 4.5 nm^2, except for the grey scale image, which shows the tiger skin structure at a larger scale. Starting from the vacuum situation in image A, showing the (1x2) missing-row reconstruction, we expose the surface to a high pressure of CO and 160℃(arrow 1). Via image B, showing the tiger skin pattern at larger scale (15 nm^2), we obtain image C (arrow 2): a flat metallic surface, clearly exhibiting double the density of rows, with respect to image A – the reconstruction is lifted. The reaction mechanism, on this type of surface, follows Langmuir-Hinshelwood kinetics [27, 79]. Following arrow 3 into the oxygen rich phase (image D), with $p_{CO} > \epsilon$, the surface roughens, due to the different reaction mechanism in this regime, the Mars-Van Krevelen mechanism [27, 124], as explained in the former section. As can be seen, image D exhibits the (1x2) period, consistent with the existence of the (1x2) commensurate oxide structure. When switching back to a large CO:O_2 ratio, the surface switches back to its metallic phase (arrow 4), as can be seen in image F, in which the number of rows on the surface has doubled with respect to image D. The reaction mechanism now also changes back to the Langmuir-Hinshelwood mechanism, and due to the high mobility of platinum atoms at this temperature, the surface anneals out, ending up in the same situation as image C: a flat metallic surface (arrow 5). The cycle following arrows 3-4-5 can be repeatedly reproduced. During these measurements, the transition to the incommensurate hexagonal α-PtO_2 oxide structure was not observed, nor the roughening process following this transition, because the CO pressure never dropped below ϵ.

Finally, figure 4.4 shows the CO-oxidation reaction kinetics obtained by the mass spectrometer. Graph A includes several switches from an O_2-rich to CO-rich environment. The signals, measured by the QMS for oxygen and CO, are slightly different in magnitude; the acquired oxygen signal is lower

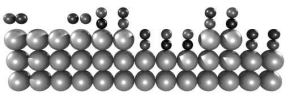

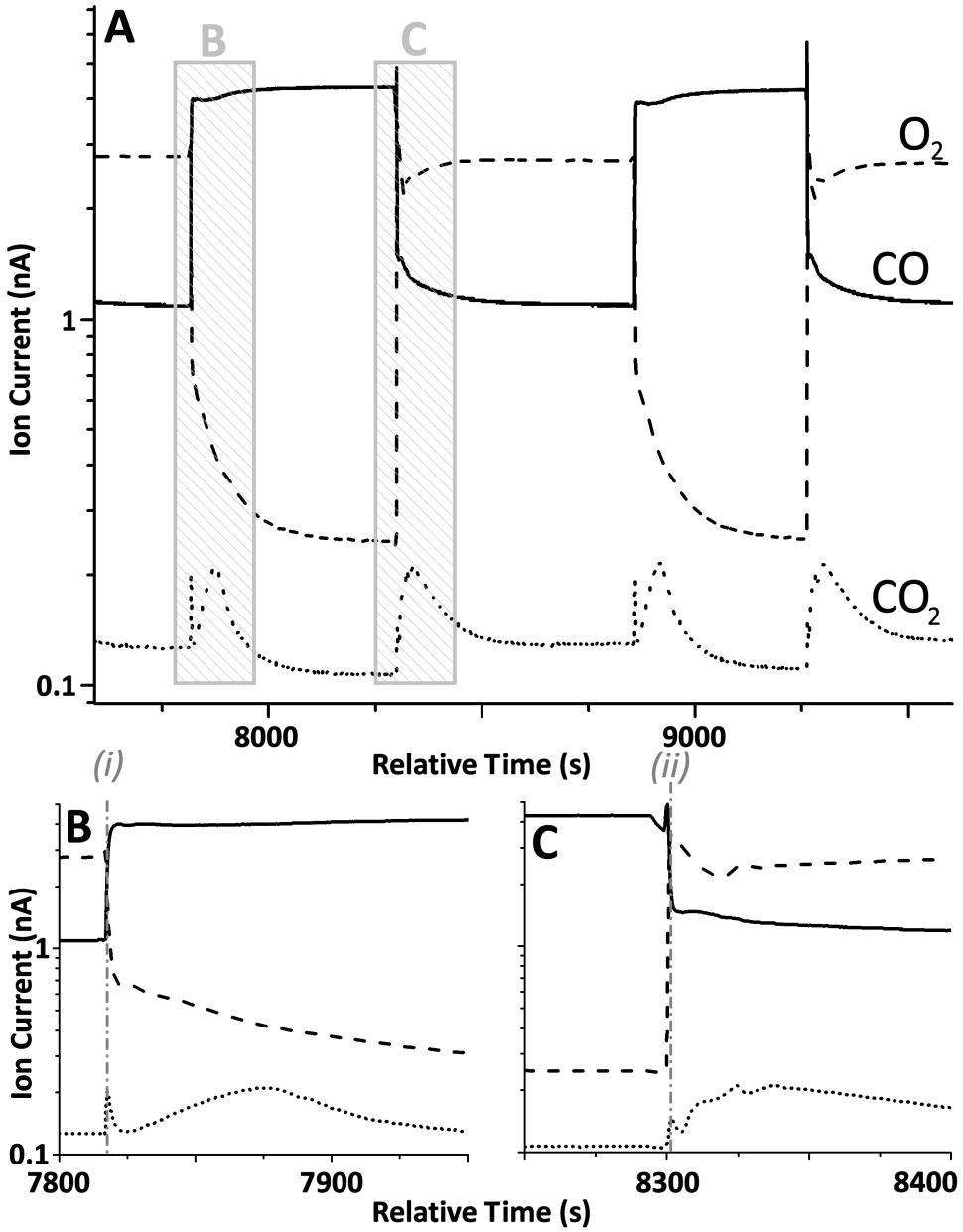

Figure 4.4: The reaction kinetics. Graph (B) and (C) are two zoom-ins of graph A, labelled by the grey rectangles.

than CO signal, for the same pressure/flow settings. This is to be expected, since the turbo pump evacuates oxygen more effectively than CO. The CO_2 signal shows some interesting features. Firstly, the steady state reaction rate, in the CO-rich environment, is lower than in the oxygen-rich environment.

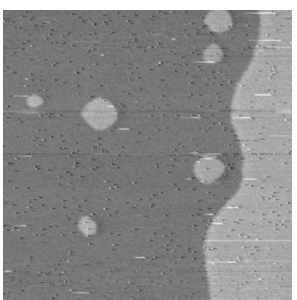

This indicates that the CO-covered metallic Pt(110) surface is less reactive than the oxidic surface, under these circumstances. Switching from oxygen-rich to CO rich, a sharp peak in the CO_2 production can be seen, as at t = 7820 s, and t = 8810 s; a zoom-in on this feature can be seen in graph B. The sharp increase might correspond to the increasing reactivity of the oxide, when offering more CO to the surface, after which the surface switches back to the metal, which, since it has a lower reactivity, causes a step down in reaction rate. The broader peaks, following these sharp peaks, are the Langmuir-Hinshelwood peaks, peaking at the optimal CO/O_2 ratio for that particular environment. On the other hand, when switching from CO to O_2, the oxidation of the surface happens on the decreasing slope of the Langmuir-Hinshelwood peak at t = 8310 s(graph C), after which the surface maintains a higher reactivity, directly proportional to the CO partial pressure. In the STM images, obtained under oxygen-rich flow conditions, the (1x2) period was always visible, indicating that the partial CO pressure, as can be seen in spectrum A of figure 4.4, under these conditions, was always sufficiently high to maintain this structure. Changing the flow reactor to a batch reactor might lead to consumption of all the available CO, during which the surface might change to its bulk α-PtO_2 phase. Deteriorating tip quality, however, prevented us from observing this transition. The next section will briefly focus on the tip quality, showing an example of the surface switching from the commensurate oxide to a metal.

4.2.2 Transition

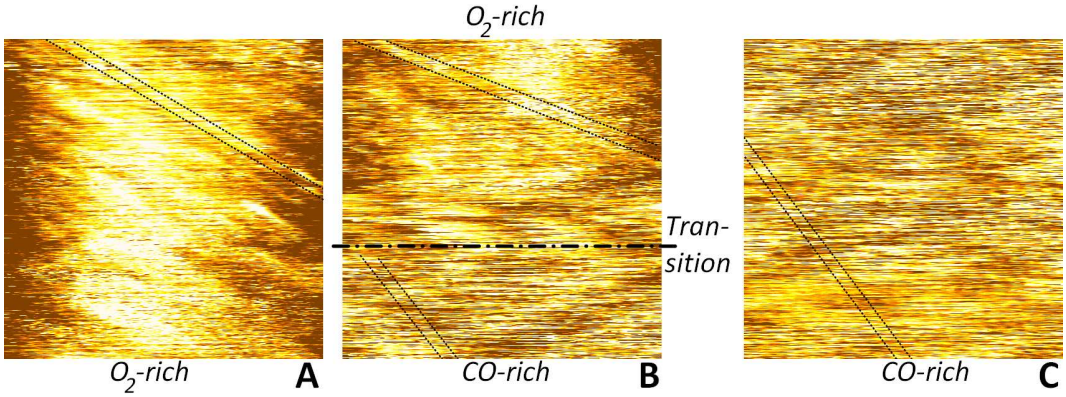

Figure 4.5: 25 nm x 25 nm STM images, showing a transition from the oxidic to the metallic terminated surface. (A) shows the oxide, (B) the transition, and (C) the metal.

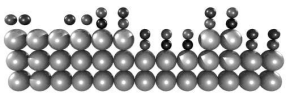

As mentioned in the last paragraph, the quality of the tip can deteriorate quickly under extreme conditions. As an example, a series of consecutive STM images is shown in figure 4.5, in which a transition from the (1x2) commensurate surface oxide to the metallic phase has been recorded. Image A shows the oxide, in which the black lines indicate the direction of the atomic rows. Image C shows the metal, in which the black lines also assist in distinguishing the barely visible atomic rows. In image B, the transition takes place at roughly two-third from the top of the image. The transition occurs at the same time that we observe a step down in reaction rate, for instance at $t = 7820$ s in figure 4.4. The reactivity of the surface oxide, under the offered high oxygen pressure conditions, is higher than the metal under similar, but high CO pressure, conditions. This step down in reaction rate also causes a small change in the thermal drift; since fewer (exothermic) reactions occur at the surface, the temperature will decrease slightly.

As can already be seen in image A, the image quality on the oxide is visibly worse than the images shown in figures 4.2 and 4.3. During the transition, visibility was completely lost, and the first images in the CO-rich environment are hardly any better. There are several reasons for this behavior. Firstly, the tip used is a mechanically sheared PtIr (80% Pt, 20% Ir) tip. In an oxidizing environment, this tip will also oxidize, which negatively influences the image quality. Moreover, the tip will also act as a catalyst for the reaction. As can be seen in image B in figure 4.2, the platinum surface exhibits a huge mobility, which will not be different on the tip. Atoms can migrate through the tip apex, leading to the horizontal stripiness in the images, due to the slow z-feedback response of the electronics, with respect to the speed at which atoms migrate through the tip apex. These horizontal stripes were observed in all our STM images, at least up to a certain level. During the switching of the gas environments, the more stoichiometric CO/O_2 ratio will lead to a changing catalytic activity of the tip, which leads to surface dynamics, making it incapable of imaging. This can clearly be seen in image B of figure 4.5, where all the details on the surface were completely lost. The tip surface possibly could also be roughened by the Mars-van Krevelen mechanism, leading to an initially rough tip surface, after switching back to a CO-rich environment; the smoothing of this surface will also lead to noise, caused by atoms passing the apex, which we observe in image C.

So in order to observe more extreme situations, such as, in this particular experiment, a change from an oxidic phase to a metallic phase, or even from one oxidic phase to another, the quality of the tip needs to be improved. One can think of using etched PtIr (or W) tips, rather than mechanically sheared

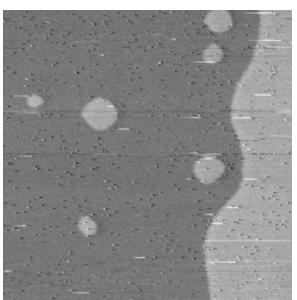

ones, and gold plating these sharp tips, to make them inert. One could even think of using tips made of pure gold, but gold is a very soft material to work with.

4.3 Conclusion and outlook

Observations on the reaction system of CO oxidation on Pt(110), making use of the ReactorSTM Mark II, support the work previously done by Hendriksen et al. and Ackermann et al. [27, 36]. The atomic row structure on the surface could be resolved in a series of gas environments, which have been divided into phases, as in figure 4.1 and 4.3, shedding light on the different surface terminations in these different phases. More directly, the (1x2) commensurate surface oxide structure, proposed by density functional theory calculations, has been imaged, and shows that this structure completely covers the surface. CO_2 reaction rates seem to be higher for the oxidized surface than for the metallic surface. All in all, as already pointed out in chapter 2, the ReactorSTM Mark II operates as intended; this experiment shows that it is capable of providing new insights into atomic-scale high-pressure, high-temperature catalysis, bringing many unexplored areas within striking distance.

For future STM experiments, it is necessary to improve the quality of the tip. The possibilities of gold plating tip and reactor compatible materials, to improve stability, are currently being explored. This step is also necessary to improve imaging in future experiments, including other strongly oxidizing or aggressive agents, such as NO and H_2S.